

Abstract of doctoral thesis

Charge transport in strongly disordered solids

Towards the Anderson metal-insulator transition

Jindřich Kolorenč

Faculty of Mathematics and Physics, Charles University, Prague, 2004

Výsledky tvořící disertaci byly získány během prezenčního doktorského studia na MFF UK v Praze ve spolupráci s FZÚ AV ČR v letech 2000–2004.

Disertant: Mgr. Jindřich Kolorenč
Fyzikální ústav AV ČR,
Na Slovance 2, 182 21 Praha 8

Školitel: Prof. RNDr. Václav Janiš, DrSc.
Fyzikální ústav AV ČR,
Na Slovance 2, 182 21 Praha 8

Konzultant: RNDr. Václav Špička, CSc.
Fyzikální ústav AV ČR,
Cukrovarnická 10, 162 53 Praha 6

Školící pracoviště: Fyzikální ústav AV ČR,
Na Slovance 2, 182 21 Praha 8

Oponenti: Prof. RNDr. Bedřich Velický, CSc.
Matematicko-fyzikální fakulta UK,
Ke Karlovu 5, 121 16 Praha 2

RNDr. Peter Markoš, CSc.
Fyzikálny ústav SAV,
Dúbravská cesta 9, 845 11 Bratislava 45

Předseda RDSO F1: Prof. RNDr. Jiří Bičák, DrSc.
Matematicko-fyzikální fakulta UK,
V Holešovičkách 2, 180 00 Praha 8

Autoreferát byl rozeslán dne

Obhajoba disertace se koná dne před komisí pro obhajoby disertačních prací v oboru F1 “Teoretická fyzika, astronomie a astrofyzika” na MFF UK, Ke Karlovu 3, Praha 2 v místnosti č. 105. S disertací je možno se seznámit na studijním oddělení pro doktorské studium na MFF UK, Ke Karlovu 3, Praha 2.

Contents

1	Charge transport in disordered solids	3
2	Objectives of the thesis	5
3	Diffusion of electrons	7
4	Two-particle Green function	9
4.1	Bethe-Salpeter equations	9
4.2	Parquet equation	11
4.3	Time-reversal invariance	11
5	Limit to high spatial dimensions	12
6	Mean-field theory of the Landau type	14
7	Weighted diffusion pole vs. conservation laws	16
8	Conclusions	19

1. Charge transport in disordered solids

Among thermodynamic and kinetic characteristics of materials the electrical conductivity plays a relatively important role. Virtually everyone knows Ohm's law which is rather easy to observe experimentally. On the other hand, theoretical insight into transport properties of solids meets a fundamental difficulty already at first stages of the investigation. The notion of non-interacting electrons in a perfect, translationally invariant lattice, so helpful in other areas of solid state physics, is not appropriate here as it yields unphysical zero value of resistivity. In order to achieve meaningful results, some processes slowing down the electron motion have to be taken into account. This thesis focuses on an electron gas in impure metals where scatterings of electrons on lattice imperfections (impurities) represent an important contribution to nonzero resistivity. In particular, this mechanism is the dominant one at low temperatures where the effects of lattice vibrations (phonons) become negligible.

The simplest theoretical description of electronic transport was proposed by Drude. It is built on a classical concept, according to which charge carriers (electrons) are supposed to move freely between successive collisions with randomly distributed scattering centers, τ being the average time separating these scattering events (see Figure 1). Such a picture yields the static electrical conductivity of the well known form

$$\sigma = \frac{ne^2}{m} \tau \quad (1)$$

where n , e and m stand for concentration, charge and mass of conduction electrons, respectively [1]. The Drude conductivity formula (1) can be re-derived even when the

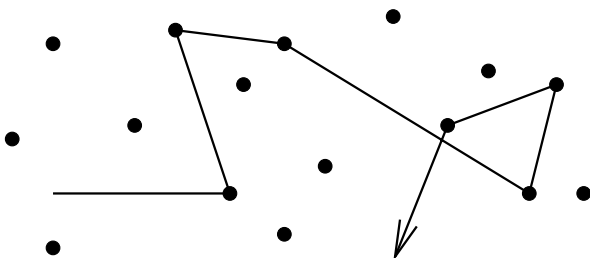
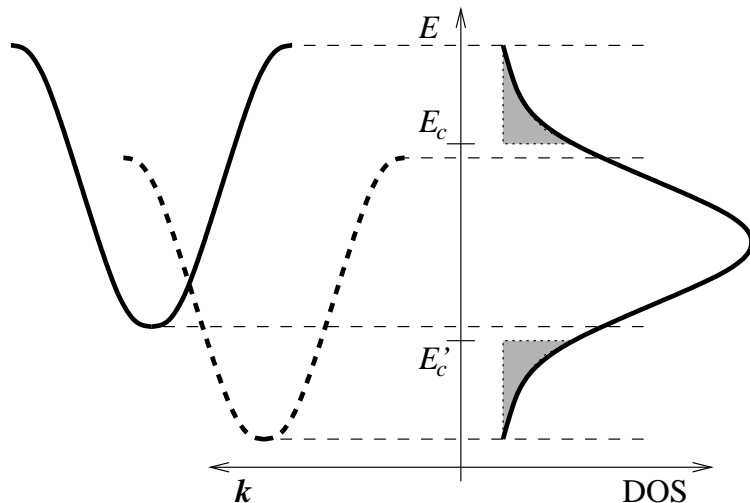


Figure 1: Piecewise motion of a classical particle in a random potential. The average time between individual scatterings is τ .

Figure 2: Two-component substitutional alloy in three dimensions. In the left part, the two energy dispersion relations corresponding to *clean* components are sketched. In the right part, the alloy density of electronic states is drawn. The wavefunctions from the center of the band are extended, whereas at band edges, in the so-called Lifshitz tails (filled regions in the graph), the electron eigenstates are localized.



electrons obey quantum-mechanical laws and not classical equations of motion that were assumed by Drude. The verbal interpretation of the underlying physics then is that due to scatterings on impurities the electron eigenstates of an ideal lattice (the Bloch waves that are *extended* through the whole sample) have a finite lifetime, τ , instead of an infinite one which corresponds to a perfect crystal.

The Drude theory works quite well at high temperatures. If a disordered system is cooled down, quantum coherence causes the disorder to influence the electron motion more dramatically. Anderson discovered [2] that a sufficiently strong disorder may give rise to such a destructive interference of scattered electron waves that they change from extended to spatially confined. Envelopes of such *localized* wavefunctions have exponentially decaying tails,

$$|\psi(\mathbf{r})| \sim \exp(-|\mathbf{r} - \mathbf{r}_0|/\xi) \quad (2)$$

where \mathbf{r}_0 is a point in space around which the eigenstate is localized. The parameter ξ controls spatial extension of the wavefunction and is called *localization length*. The localization effects substantially depend on dimensionality of the system under investigation. They are most pronounced in one dimension where it can be rigorously shown that *all* electron eigenstates are localized for arbitrarily weak disorder [3]. Therefore, infinitely long quantum wires are insulators. In higher dimensions almost no rigorous results are known. Some evidence has been amassed, based on a scaling hypothesis [4] or on a self-consistent diagrammatic method [5], indicating that even in two dimensions all electron states are localized, no matter how weak the disorder is. In the same time, experimental data for both metallic and insulating behavior in 2D samples very close to $T = 0$ K were presented [6]. Attempts to explain such measurements suggest possible insufficiency of one-particle theories, whereto References 4 and 5 belong, and maintain importance of electron-electron interactions in *realistic* situations [7].

In three-dimensional lattices the electronic density of states (DOS) has a structure as depicted in Figure 2. The electron eigenstates located close to the band edges, in the so-called *Lifshitz tails*, are localized, whereas those belonging to the energy interval around the band center are extended. The energies where the character of wavefunctions changes are referred to as *mobility edges*. In Figure 2 we denote them E_c , respectively E'_c . At these points the transport behavior goes over from metallic to insulating, i. e., the

metal-insulator transition (MIT)¹ takes place there. As the disorder strength grows, the mobility edges E_c and E'_c move towards the band center where they eventually meet and the whole band becomes localized. Such a scenario, originally based on more or less intuitive arguments, was later rigorously confirmed [8].

An insight into localized states in the Lifshitz tails may be won on a simple example of a binary alloy [9]. It can be shown that the density of states of such an alloy is nonzero for all energies where either one of the densities of states corresponding to respective clean crystals is nonzero, Figure 2. However, outside the intersection of the two clean spectra the alloy density of states is rather small in magnitude. The electron wavefunctions contributing to these tails come from such disorder configurations, in which large islands of one component exist that are immersed, far one from another, into a typical configuration of atoms in the lattice. In this way we are led to the conclusion that the Lifshitz tails are built up of states *bound* to these rare fluctuations of the spatial distribution of alloy components. The closer to the alloy band edge the eigenenergy of such a bound state lies, the larger, and thus less probable, is the corresponding fluctuation.

The transition from extended to localized states is not the only change that occurs in the electronic spectrum as the disorder increases. When the alloy constituents are different enough, the respective clean bands do not overlap and the alloy band is split into two subbands. Considering this fact we may ask whether the whole band becomes localized first and only then splits or if the inverse scenario applies.

Understanding the electron dynamics in three-dimensional disordered lattices is only qualitative at present. There exists no reliable theory providing *quantitative* estimates for positions of mobility edges etc. Several approximation schemes, both analytical [10] and numerical [11, 12], were developed to calculate quasi-particle spectra in disordered crystals. The numerical approaches lie outside the scope of this thesis and will not be discussed. Out of the analytical methods, the coherent-potential approximation (CPA) turned out to be the most successful. For the binary alloy model introduced above it predicts the anticipated opening of a band gap for large differences between constituents [13]. On the other hand, the CPA is not able to reproduce the correct bandwidth. Moreover, when the CPA is applied to transport properties [14], it corresponds more or less to the simple Drude concept and contains no signs of quantum corrections.

2. Objectives of the thesis

The objective of the thesis is to construct an approximation scheme that inherits the properties of the coherent-potential approximation and, in the same time, contains non-trivial quantum corrections to the semi-classical values of transport coefficients. These corrections, which are absent in the CPA, originate in the inter-site phase coherence that enhances backward scatterings. Predictions of the demanded theory should comply with the phenomenological expectations listed above, i. e., the quantum phenomena should be most pronounced at the band edges and in the contingent impurity band. It will be demonstrated that the mean-field-like approximation developed in the thesis really

¹Several types of metal-insulator transitions are distinguished in the literature. Here we discuss the Anderson MIT which is caused by disorder. Mott demonstrated that a transition from metallic to insulating regime can also be driven by electron-electron interactions. Such a phenomenon is called Mott MIT.

behaves in that way. Furthermore, since the approximation is self-consistent, it allows us to access not only corrections of a perturbative character, but non-perturbative effects as well. The non-perturbative phenomenon that we are heading for is the Anderson metal-insulator transition.

The model we study is the original Anderson model [2], the Hamiltonian of which reads

$$\hat{H} = \sum_{i,j} t_{ij} \hat{c}_i^\dagger \hat{c}_j + \sum_i V_i \hat{c}_i^\dagger \hat{c}_i \quad (3)$$

where \hat{c}_i^\dagger and \hat{c}_i create and annihilate, respectively, an electron on lattice site i . The matrix t_{ij} describes probability of a particle hopping from site j to site i . In the simplest version only hoppings between nearest neighbors are allowed, $t_{ij} = t\delta_{|i-j|,1}$. The local energies V_i are random, characterized by a probability distribution $P(V_i)$. The distribution function $P(V_i)$ is the same for all lattice sites without any correlations between them.

A direct analysis of the Anderson Hamiltonian (3) is possible only by numerical means, since it has too many parameters (the on-site potentials V_i) and lacks any apparent symmetry that would help with their reduction. As we want to tackle the problem analytically, we perform averaging over all possible disorder configurations that restores the translational invariance obeyed by a clean (non-disordered) lattice. The configurational average $\langle F \rangle_{av.}$ of a function of on-site potentials $F(V_i, V_j, V_k, \dots)$ is defined as

$$\langle F \rangle_{av.} = \frac{1}{N_C} \sum_{\{configurations\}} F(V_i, V_j, V_k, \dots) \quad (4)$$

where N_C is the total number of disorder configurations compatible with a given macroscopic constraint such as fixed impurity concentration. The restoration of the translational invariance has its price — the averaging procedure transforms the original system of non-interacting electrons to an ensemble of correlated particles. However, we gain more than we lose as the artificial interacting system can be studied with the aid of standard many-body diagrammatic techniques, which is the method utilized in the thesis.

We start with classification of two-particle diagrams into topologically distinct scattering channels that allows us to formulate self-consistent equations for two-particle Green functions (parquet scheme). Consequently, an asymptotic limit to high spatial dimensions, i. e. the standard “generator” of mean-field theories, is employed for systematic construction of approximate solutions of the parquet equations. In the strict limit $d = \infty$ only terms of the order $O((1/d)^0)$ contribute and a simple sum of the CPA and the so-called *weak localization* correction [15, 16] is obtained. A further self-consistent inclusion of $O(1/d)$ terms leads to an advanced approximation scheme that predicts vanishing of the electrical conductivity above a certain critical disorder strength in any finite spatial dimensions.

In the course of developing our mean-field-like solution a crucial difficulty is encountered — we are not able to comply with the particle number conservation law. In other words, Ward identities for configurationally averaged Green functions are not fulfilled to the extent that is nowadays widely assumed. However, it can be demonstrated that the violation of Ward identities is not an artifact of our approximations. On the contrary, it is inevitable in principle. It turns out that the particle number non-conservation is only virtual and can be understood if the configurational averaging is reexamined. The

conclusion is that only extended states can survive the averaging procedure and that localized states are lost already during this very early step of the theoretical description of electrons moving in a random potential.

3. Diffusion of electrons

The electron transport we aim to describe falls among (weakly) non-equilibrium phenomena. Therefore, the proper means to study the physical system of our interest — many non-interacting electrons on an impure lattice — is to utilize the linear response theory [17,18]. This is the path we follow in Chapter 2 of the thesis where the formalism for calculation of transport properties of disordered systems is introduced. In this paragraph we use a “short cut” starting from quantum mechanics of a single electron. Such an approach is not as comprehensive as the one of the linear response theory, but it is likely to provide cleaner physical insight.

The wavefunction of an electron on a lattice can be written as $|\psi(t)\rangle = \sum_j \psi_j(t)|j\rangle$ where $|j\rangle$ are on-site orbitals (Wannier functions) localized at positions \mathbf{R}_j . If we start with a particle located at site i , i. e., if its wavefunction at time $t = 0$ has a simple form $\psi_j(0) = \delta_{ij}$, then at later times, $t > 0$, the wavefunction $\psi_j(t)$ and the corresponding particle density $n_j(t)$ read

$$\psi_j(t) = \langle j | e^{-i\hat{H}t} | i \rangle \quad \text{and} \quad n_j(t) = \psi_j(t) \psi_j^*(t) = \langle j | e^{-i\hat{H}t} | i \rangle \langle i | e^{i\hat{H}t} | j \rangle. \quad (5)$$

For the given initial condition, $\psi_j(0) = \delta_{ij}$, the particle density is given solely by the transfer probability $\mathcal{P}_{ji}(t)$,

$$n_j(t) = \mathcal{P}_{ji}(t) = \theta(t) \langle j | e^{-i\hat{H}t} | i \rangle \langle i | e^{i\hat{H}t} | j \rangle. \quad (6)$$

The Heaviside step function was introduced to ensure analyticity of the Fourier transform of \mathcal{P}_{ji} from time to frequency. It is tempting to generalize the above equation to a form $n_j(t) = \sum_i \mathcal{P}_{ji}(t)n_i(0)$ that is incorrect, however. Classical quantities, such as the density n_i , do not carry all the quantum-mechanical information.

A direct evaluation of expression (6) is inconvenient, more feasible is to work with the frequency representation of the probability \mathcal{P}_{ji} . If we introduce retarded and advanced Green functions as Fourier transforms of matrix elements of the evolution operator,

$$\mathcal{G}_{ji}^R(E) = -i \int_0^\infty dt e^{i(E+i0)t} \langle j | e^{-i\hat{H}t} | i \rangle = \left\langle j \left| \frac{1}{E + i0 - \hat{H}} \right| i \right\rangle, \quad (7a)$$

$$\mathcal{G}_{ji}^A(E) = i \int_{-\infty}^0 dt e^{i(E-i0)t} \langle j | e^{-i\hat{H}t} | i \rangle = \left\langle j \left| \frac{1}{E - i0 - \hat{H}} \right| i \right\rangle, \quad (7b)$$

then the Fourier transform of the transfer probability \mathcal{P}_{ji} is represented as a convolution of these two Green functions,

$$\mathcal{P}_{ji}(t) = \frac{1}{2\pi} \int_{-\infty}^\infty d\omega e^{-i\omega t} \mathcal{P}_{ji}(\omega) \quad \text{where} \quad \mathcal{P}_{ji}(\omega) = \frac{1}{2\pi} \int_{-\infty}^\infty dE \mathcal{G}_{ji}^R(E + \omega) \mathcal{G}_{ij}^A(E). \quad (8)$$

So far, the probability \mathcal{P}_{ji} as well as the one-particle Green functions \mathcal{G}_{ji}^R and \mathcal{G}_{ji}^A depend on a particular configuration of disorder, i. e. on one individual choice of local potentials V_i in the Anderson model (3). The quantities \mathcal{P}_{ji} , \mathcal{G}_{ji}^R and \mathcal{G}_{ji}^A are quite complex,

since they do not display any apparent symmetry that would help treat them. It is the next step — averaging over all disorder configurations (4) — that makes these functions maintainable. Configurational averaging is not only a technically motivated procedure (it restores translational invariance), but has a direct physical content as well, since it provides reproducibility (sample independence) of final results.

Averaging of the probability expression (8) introduces the two-particle Green function $G_{jk,il}^{(2)}(z_1, z_2) \equiv \langle \mathcal{G}_{ji}(z_1) \mathcal{G}_{lk}(z_2) \rangle_{\text{av.}}$. It is a nontrivial quantity as an average of a product generally differs from a product of averages. Due to gained translational invariance the two-particle Green function depends only on differences of its site indices, moreover, only three of these differences are independent. This property allows for a threefold Fourier transform to momentum space,

$$G_{\mathbf{k}\mathbf{k}'}^{(2)}(z_1, z_2; \mathbf{q}) = \frac{1}{N} \sum_{ijkl} e^{i(\mathbf{k}+\mathbf{q})\cdot\mathbf{R}_i} e^{-i\mathbf{k}\cdot\mathbf{R}_l} e^{-i(\mathbf{k}'+\mathbf{q})\cdot\mathbf{R}_j} e^{i\mathbf{k}'\cdot\mathbf{R}_k} G_{jk,il}^{(2)}(z_1, z_2) \quad (9)$$

where N stands for the total number of lattice sites. The diagrammatic representation we use for the two-particle Green function is

The diagram shows two representations of the two-particle Green function $G^{(2)}$. On the left, the direct space representation is a square box labeled $G^{(2)}$ with four external legs: top-left z_1, i , top-right z_1, j , bottom-left z_2, l , and bottom-right z_2, k . On the right, the momentum space representation is a similar square box labeled $G^{(2)}$ with four external legs: top-left $z_1, \mathbf{k} + \mathbf{q}$, top-right $z_1, \mathbf{k}' + \mathbf{q}$, bottom-left z_2, \mathbf{k} , and bottom-right z_2, \mathbf{k}' . The two diagrams are separated by the word "and".

in direct and momentum space, respectively.

At this point we return from one particle on a lattice back to the many-fermion systems we intend to investigate. At low temperatures the electron gas is degenerate and only a small fraction of electrons, having energies close to the Fermi level E_F , can participate in weakly non-equilibrium phenomena such as diffusion. Out of the whole integral in formula (8) only a narrow vicinity of the Fermi energy survives,

$$P_{ji}(\omega) = \langle \mathcal{P}_{ji}(\omega) \rangle_{\text{av.}} \approx \phi_{ji} \Delta E = \frac{\Delta E}{2\pi} G_{jj,ii}^{RA}(E_F + \omega, E_F). \quad (11)$$

Parameter ΔE measures extension of the relevant energy interval around E_F . In the same time, the quantity ΔE controls “distance” of our transport state from the equilibrium one. The differential transfer probability ϕ_{ji} describes relaxation of non-equilibrium particle density variations and will thus be referred to as *density relaxation function*. Its momentum representation is given by a trace of the two-particle Green function,

$$\phi(\omega, \mathbf{q}) = \frac{1}{N} \sum_{ij} e^{i\mathbf{q}\cdot\mathbf{R}_i} e^{-i\mathbf{q}\cdot\mathbf{R}_j} \phi_{ji}(\omega) = \frac{1}{2\pi} \frac{1}{N^2} \sum_{\mathbf{k}\mathbf{k}'} G_{\mathbf{k}\mathbf{k}'}^{RA}(E_F + \omega, E_F; \mathbf{q}). \quad (12)$$

In terms of Feynman diagrams the relaxation function is visualized, in direct and momentum space, as

The diagram shows two representations of the relaxation function G^{RA} . On the left, the direct space representation is a horizontal oval shape labeled G^{RA} with two external legs: left i and right j . On the right, the momentum space representation is a similar horizontal oval shape labeled G^{RA} with four external legs: top-left $\mathbf{k} + \mathbf{q}$, top-right $\mathbf{k}' + \mathbf{q}$, bottom-left \mathbf{k} , and bottom-right \mathbf{k}' . The two diagrams are separated by the word "and".

The quasi-classical diffusive relaxation of density inhomogeneities corresponds to small frequency and small momentum asymptotics of the density relaxation function ϕ having a singular form

$$\phi(\omega, \mathbf{q}) \approx \frac{g_F}{-i\omega + Dq^2}, \quad D > 0. \quad (14)$$

This singularity is called *diffusion pole*. The newly introduced quantities are the diffusion constant D and the density of electronic states at the Fermi energy $g_F = g(E_F)$. In the following paragraphs we seek a systematic method for approximate evaluation of the two-particle Green function in order to access the $\omega, \mathbf{q} \rightarrow 0$ asymptotics of the relaxation function ϕ by a fully quantum means. Having such an approximation scheme in hand we will be able to reliably describe behavior of small density variations even in the case of the strong disorder limit where quantum coherence effects are expected to play a crucial role. The key questions to answer are: how the diffusion constant D evolves with increasing disorder and how the diffusion pole changes as the Anderson localization transition is approached.

4. Two-particle Green function

As demonstrated above, in order to characterize the electron motion on disordered lattices we need to evaluate the configurationally averaged two-particle Green function. It is useful to come over from the full Green function $G^{(2)}$ to a two-particle vertex Γ defined by a decomposition

$$G_{\mathbf{k}\mathbf{k}'}^{(2)}(\mathbf{q}) = N\delta_{\mathbf{k}\mathbf{k}'} G_1(\mathbf{k} + \mathbf{q})G_2(\mathbf{k}) + G_1(\mathbf{k} + \mathbf{q})G_2(\mathbf{k}) \Gamma_{\mathbf{k}\mathbf{k}'}(\mathbf{q}) G_1(\mathbf{k}' + \mathbf{q})G_2(\mathbf{k}'). \quad (15)$$

The vertex Γ is just the two-particle Green function with the uncorrelated part subtracted. Quantity $G(z, \mathbf{k})$ is Fourier transform of the averaged one-particle Green function,

$$G(z, \mathbf{k}) = \frac{1}{N} \sum_{ij} e^{i\mathbf{k}\cdot\mathbf{R}_i} e^{-i\mathbf{k}\cdot\mathbf{R}_j} \langle \mathcal{G}_{ji}(z) \rangle_{av}. \quad (16)$$

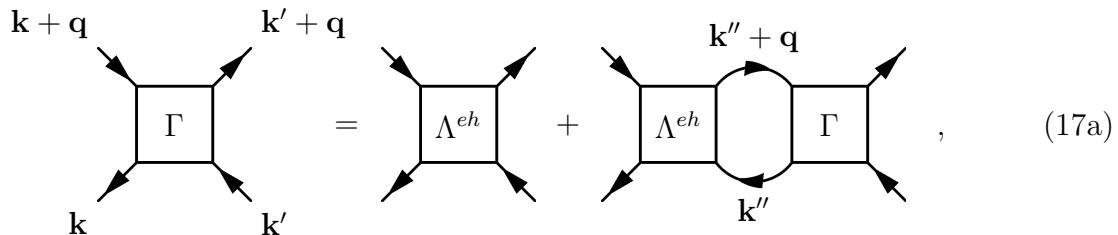
We suppressed the energies z_1 and z_2 in equation (15), since they are not dynamical variables and act only as external parameters. They are easily deducible from one-electron propagators $G_{1,2}(\mathbf{k}) = G(z_{1,2}, \mathbf{k})$.

4.1. Bethe-Salpeter equations

The method we choose for evaluation of one- and two-particle Green functions is the diagrammatic perturbation expansion. Since we aim to the disorder-driven metal-insulator transition that clearly falls among non-perturbative phenomena, we need to sum up infinitely many terms in the perturbation series. A convenient way to do so is to select *two-particle irreducible* diagrams (diagrams that cannot be split into two parts by cutting two fermion lines) and then generate the rest of the two-particle diagrams, the so-called *reducible* contributions, with the aid of Bethe-Salpeter equation.

There is not a unique way to define two-particle irreducibility and, correspondingly, there is not only one Bethe-Salpeter equation. One possibility is to single out diagrams that do not decompose into two parts if the two fermion lines we cut have opposite

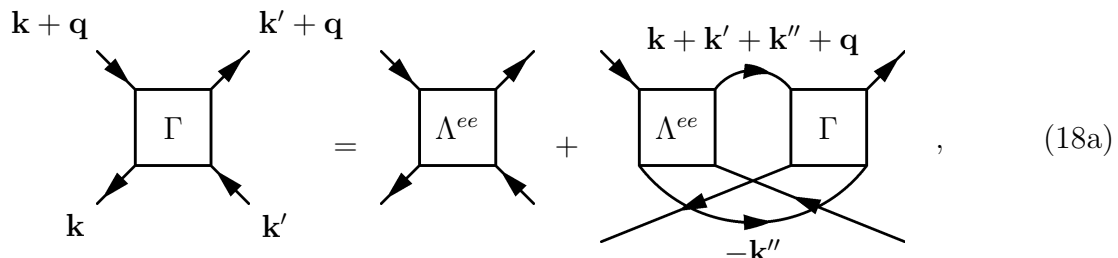
directions, i. e. one of them corresponds to an electron and the other to a hole. Such diagrams are called *electron-hole irreducible* and their sum forms the so-called electron-hole irreducible vertex Λ^{eh} . The Bethe-Salpeter equation that generates the electron-hole reducible diagrams, sum of which is $\Gamma - \Lambda^{eh}$, reads



$$\Gamma_{\mathbf{k}\mathbf{k}'}(\mathbf{q}) = \Lambda_{\mathbf{k}\mathbf{k}'}^{eh}(\mathbf{q}) + \Lambda_{\mathbf{k}\mathbf{k}''}^{eh}(\mathbf{q}) G_1(\mathbf{k}'' + \mathbf{q}) G_2(\mathbf{k}'') \Gamma_{\mathbf{k}''\mathbf{k}'}(\mathbf{q}). \quad (17a)$$

$$\Gamma_{\mathbf{k}\mathbf{k}'}(\mathbf{q}) = \Lambda_{\mathbf{k}\mathbf{k}'}^{eh}(\mathbf{q}) + \frac{1}{N} \sum_{\mathbf{k}''} \Lambda_{\mathbf{k}\mathbf{k}''}^{eh}(\mathbf{q}) G_1(\mathbf{k}'' + \mathbf{q}) G_2(\mathbf{k}'') \Gamma_{\mathbf{k}''\mathbf{k}'}(\mathbf{q}). \quad (17b)$$

Another way to separate reducible and irreducible diagrams is to utilize the *electron-electron (hole-hole) irreducibility*, in which the two cut fermion lines point in the same direction. The corresponding irreducible vertex we denote Λ^{ee} . The Bethe-Salpeter equation in this electron-electron scattering channel has a form



$$\Gamma_{\mathbf{k}\mathbf{k}'}(\mathbf{q}) = \Lambda_{\mathbf{k}\mathbf{k}'}^{ee}(\mathbf{q}) + \Lambda_{-\mathbf{k}'',\mathbf{k}'}^{ee}(z_1, z_2; \mathbf{q} + \mathbf{k} + \mathbf{k}'') \times G_1(\mathbf{k} + \mathbf{k}' + \mathbf{k}'' + \mathbf{q}) G_2(\mathbf{k}'') \Gamma_{\mathbf{k},-\mathbf{k}''}(\mathbf{q} + \mathbf{k}' + \mathbf{k}''). \quad (18a)$$

$$\Gamma_{\mathbf{k}\mathbf{k}'}(\mathbf{q}) = \Lambda_{\mathbf{k}\mathbf{k}'}^{ee}(\mathbf{q}) + \frac{1}{N} \sum_{\mathbf{k}''} \Lambda_{-\mathbf{k}'',\mathbf{k}'}^{ee}(z_1, z_2; \mathbf{q} + \mathbf{k} + \mathbf{k}'') \times G_1(\mathbf{k} + \mathbf{k}' + \mathbf{k}'' + \mathbf{q}) G_2(\mathbf{k}'') \Gamma_{\mathbf{k},-\mathbf{k}''}(\mathbf{q} + \mathbf{k}' + \mathbf{k}''). \quad (18b)$$

In the problem of non-interacting disordered electrons one can identify one more type of two-particle irreducibility [19]. We do not write down this *vertical* scattering channel explicitly as it is not relevant for analysis of the electron diffusion.

When using Bethe-Salpeter equation as a base for an approximation scheme, the corresponding irreducible vertex, let us choose Λ^{eh} , serves as an input that controls quality of the approximation. Even if only the lowest order term (a single diagram) is included into Λ^{eh} , the full vertex Γ contains infinitely many diagrams known as electron-hole ladders. Unfortunately, such level of approximation does not show to be very rich. It provides just the quasi-classical Drude value for the diffusion constant. We hence have to go one step further and construct self-consistent equations for the irreducible vertices Λ^{eh} and Λ^{ee} so that already these vertex functions comprehend infinitely many diagrams. It is the topological nonequivalence of the Bethe-Salpeter equations (17) and (18) that helps us manage this task.

4.2. Parquet equation

The key observation leading towards the demanded equations for the irreducible vertices is that a diagram reducible in one scattering channel is irreducible in the other channels. In terms of sets of diagrams corresponding to the vertices Λ^{eh} , Λ^{ee} and Γ this statement reads $\Gamma - \Lambda^{ee} \subset \Lambda^{eh}$. Starting from such a set relation it is quite straightforward to come to the so-called *parquet equation* [19, 20, 21]

$$\Gamma_{\mathbf{k}\mathbf{k}'}(\mathbf{q}) = \Lambda_{\mathbf{k}\mathbf{k}'}^{eh}(\mathbf{q}) + \Lambda_{\mathbf{k}\mathbf{k}'}^{ee}(\mathbf{q}) - I_{\mathbf{k}\mathbf{k}'}(\mathbf{q}) \quad (19)$$

where I denotes a two-particle vertex that is irreducible in both involved scattering channels, $I = \Lambda^{eh} \cap \Lambda^{ee}$. This vertex will be referred to as *completely irreducible*. With the aid of the parquet equation (19), the full vertex Γ can be evaluated employing the two Bethe-Salpeter equations (17) and (18) simultaneously. The “external” diagrammatic input is no longer the irreducible vertex Λ^{eh} (or Λ^{ee}), but the completely irreducible vertex I . Approximating this input by the single lowest order diagram we end up with Γ of a considerably richer structure than the sum of ladders that is achieved by inserting the same simplest diagram into Λ^{eh} (or Λ^{ee}).² The price we pay for this improvement is that now we have to solve two coupled non-linear integral equations (the Bethe-Salpeter equations) instead of just one. However, considering an additional symmetry, the time-reversal invariance, this pair of equations can be reduced to a single equation again.

4.3. Time-reversal invariance

In the case of no external magnetic fields present, the Anderson model (3) is invariant with respect to time reversal. The time inversion in non-interacting systems is expressed as inversion of the particle propagation, $\mathbf{k} \rightarrow -\mathbf{k}$, i. e., the electron and hole interchange their roles. The time-reversal invariance then means that $G(z, \mathbf{k}) = (\mathcal{T}G)(z, \mathbf{k}) \equiv G(z, -\mathbf{k})$. The action of the time-inversion operator \mathcal{T} on a generic two-particle function F is shown to be $(\mathcal{T}F)_{\mathbf{k},\mathbf{k}'}(\mathbf{q}) \equiv F_{-\mathbf{k}',-\mathbf{k}}(\mathbf{q} + \mathbf{k} + \mathbf{k}')$. Alike the one-particle Green function G , the full two-particle vertex Γ is invariant with respect to \mathcal{T} , $(\mathcal{T}\Gamma)_{\mathbf{k},\mathbf{k}'}(\mathbf{q}) = \Gamma_{\mathbf{k},\mathbf{k}'}(\mathbf{q})$. On the other hand, the irreducible vertices Λ^{eh} and Λ^{ee} do not stay untouched under the time inversion. Actually, they transform onto each other,

$$(\mathcal{T}\Lambda^{eh})_{\mathbf{k},\mathbf{k}'}(\mathbf{q}) = \Lambda_{\mathbf{k},\mathbf{k}'}^{ee}(\mathbf{q}) \quad \text{and} \quad (\mathcal{T}\Lambda^{ee})_{\mathbf{k},\mathbf{k}'}(\mathbf{q}) = \Lambda_{\mathbf{k},\mathbf{k}'}^{eh}(\mathbf{q}). \quad (20)$$

The same holds for the Bethe-Salpeter equations (17) and (18), the electron-hole scattering channel changes to the electron-electron one and vice versa. This property allows us to replace one of the Bethe-Salpeter equations in the set (17), (18) and (19), determining the vertices Λ^{eh} , Λ^{ee} and Γ as functionals of I , with one of the “mixing” relations (20). Doing so we finally come to a single integral equation to solve,

$$\Lambda_{\mathbf{k}\mathbf{k}'}^{ee}(\mathbf{q}) = I_{\mathbf{k}\mathbf{k}'}(\mathbf{q}) + \frac{1}{N} \sum_{\mathbf{k}''} \Lambda_{-\mathbf{k}'',-\mathbf{k}}^{ee}(\mathbf{q} + \mathbf{k} + \mathbf{k}'') G_1(\mathbf{k}'' + \mathbf{q}) G_2(\mathbf{k}'') \times [\Lambda_{-\mathbf{k}',-\mathbf{k}''}^{ee}(\mathbf{q} + \mathbf{k}' + \mathbf{k}'') + \Lambda_{\mathbf{k}'',\mathbf{k}'}^{ee}(\mathbf{q}) - I_{\mathbf{k}'',\mathbf{k}'}(\mathbf{q})]. \quad (21)$$

²The diagrams building up this advanced approximation of the vertex Γ are called parquet diagrams. The name describes the two-dimensional, area-covering character of these diagrams if they are drawn in a certain specific way.

Having Λ^{ee} , the full vertex is easily found from the parquet equation (19) written in a form $\Gamma = \mathcal{T}\Lambda^{ee} + \Lambda^{ee} - I$ that was used already in the square brackets in equation (21).

5. Limit to high spatial dimensions

The fundamental equation (21) is far too complicated to be solved exactly and we have to resort to an approximate treatment. Usually, the first attempt to introspect properties of a complex problem is construction of a mean-field approximation. Such a step may be quite straightforward in the case of classical systems, consider e. g. the Weiss solution of the Ising model of ferromagnets. Quantum fermionic systems are, on the contrary, not so easy to tackle as it is not clear what are the relevant parameters that have to be retained in the demanded simplified description. If plausible physical arguments suggesting a proper reduction of a given problem cannot be found, one needs a robust and systematic method that would replace the lacking intuition. A technique that proved successful in this field is the limit to high spatial dimensions [22, 23, 24]. The recipe is: solve the problem in the asymptotic limit $d \rightarrow \infty$, the achieved result will behave as a mean-field approximation when applied to finite dimensions, say $d = 3$. For example, if these guidelines are followed for the Ising model, the Weiss solution emerges. It is one of the most important achievements of this thesis that we are able to solve the above equation (21) asymptotically exactly in the limit $d \rightarrow \infty$, and thus to find a mean-field approximation of the full vertex Γ .

In the course of approaching the limit $d \rightarrow \infty$, the hopping parameter t of the tight-binding Hamiltonian (3) has to be rescaled, $t \rightarrow t d^{-1/2}$, in order to keep the dynamic balance between kinetic and potential energy [22]. The total energy of the system is not proportional to the volume in the limit $d \rightarrow \infty$ without this adjustment [25]. Due to the modified hopping, the local and non-local elements of the one-particle Green function G substantially differ. The local part, G_{ii} , remains finite in $d \rightarrow \infty$, whereas the off-diagonal (non-local) part, $\bar{G}_{ij} \equiv G_{ij} - \delta_{ij}G_{ii}$, scales as $d^{-1/2}$. In the momentum representation these relations read

$$G(z) = \frac{1}{N} \sum_{\mathbf{k}} G(z, \mathbf{k}) \sim 1 \quad \text{and} \quad \bar{G}(z, \mathbf{k}) = G(z, \mathbf{k}) - G(z) \sim d^{-1/2}. \quad (22)$$

To take advantage of this diversity it is convenient to reformulate the Bethe-Salpeter equations (17) and (18) so that the differently behaved Green function elements become naturally separated. Such a differentiation is obtained when the two-particle irreducibility is formulated only for the off-diagonal Green function \bar{G} . All diagrams containing only local elements of the one-particle Green function are then qualified as completely irreducible. The new self-consistent equation for the irreducible vertex has entirely the same form as equation (21),

$$\begin{aligned} \bar{\Lambda}_{\mathbf{k}\mathbf{k}'}^{ee}(\mathbf{q}) &= \bar{I}_{\mathbf{k}\mathbf{k}'}(\mathbf{q}) + \frac{1}{N} \sum_{\mathbf{k}''} \bar{\Lambda}_{-\mathbf{k}'', -\mathbf{k}}^{ee}(\mathbf{q} + \mathbf{k} + \mathbf{k}'') \bar{G}_1(\mathbf{k}'' + \mathbf{q}) \bar{G}_2(\mathbf{k}'') \\ &\quad \times [\bar{\Lambda}_{-\mathbf{k}', -\mathbf{k}''}^{ee}(\mathbf{q} + \mathbf{k}' + \mathbf{k}'') + \bar{\Lambda}_{\mathbf{k}''\mathbf{k}'}^{ee}(\mathbf{q}) - \bar{I}_{\mathbf{k}''\mathbf{k}'}(\mathbf{q})]. \end{aligned} \quad (23)$$

The only difference is the substitution $G, \Lambda^{eh}, \Lambda^{ee}, I \rightarrow \bar{G}, \bar{\Lambda}^{eh}, \bar{\Lambda}^{ee}, \bar{I}$ that originates in the modified definition of the two-particle irreducibility. The full vertex is still found

Now we use the high-dimensional algebra summarized above to find the asymptotic solution for the two-particle vertex Γ . From the diagrammatic analysis one can conclude that the momentum dependence of the irreducible vertices in the limit $d \rightarrow \infty$ reads $\bar{\Lambda}_{\mathbf{k}\mathbf{k}'}^{eh}(\mathbf{q}) = \sum_{n=0}^{\infty} \Lambda_n \bar{\chi}^n(\mathbf{q} + \mathbf{k} + \mathbf{k}')$ and $\bar{\Lambda}_{\mathbf{k}\mathbf{k}'}^{ee}(\mathbf{q}) = \sum_{n=0}^{\infty} \Lambda_n \bar{\chi}^n(\mathbf{q})$. Notice the explicit fulfillment of the two-particle electron-hole symmetry (20). The expansion of the coefficients Λ_n in the small parameter d^{-1} begins as $\Lambda_n = \gamma^n + O(d^{-1})$. In order to determine the $O(d^{-1})$ term we insert the aforementioned ansatz for $\bar{\Lambda}^{ee}$ into equation (23). It finally yields the vertex Γ in a form

$$\Gamma_{\mathbf{k}\mathbf{k}'}(\mathbf{q}) = \frac{\bar{\gamma}}{1 - \bar{\gamma} \bar{\chi}(\mathbf{q})} + \frac{\bar{\gamma}}{1 - \bar{\gamma} \bar{\chi}(\mathbf{k} + \mathbf{k}' + \mathbf{q})} - (2\bar{\gamma} - \gamma) \quad (29)$$

where the new quantity $\bar{\gamma}$, which in a way generalizes the CPA vertex γ , is a solution of a self-consistent equation

$$\bar{\gamma} = \gamma + \bar{\gamma} \frac{1}{N} \sum_{\mathbf{q}} \frac{\bar{\gamma}^2 \bar{\chi}^2(\mathbf{q})}{1 - \bar{\gamma} \bar{\chi}(\mathbf{q})}. \quad (30)$$

Expressions (29) and (30) represent the high-dimensional asymptotics of the full two-particle vertex Γ that is *exact* up to the order $\sim d^{-1}$.

Although the self-consistent solution (29), (30) was derived from the high-dimensional reasoning, its application is not restricted to the limit $d \rightarrow \infty$. It can be, and it is intended to be, used in any spatial dimensions as a mean-field approximation. In such a case the $d \rightarrow \infty$ limit of the “bubble” $\bar{\chi}$, standing in equations (29) and (30), is replaced with its actual d -dimensional value. Then, of course, the convolution rules (26) and (28) cannot be used to simplify the determination of the vertex $\bar{\gamma}$ from equation (30). A full d -dimensional calculation has to be performed instead.

Once we have acquired the vertex Γ we can evaluate the physical quantity of our interest — the density relaxation function ϕ . Combining equations (12), (15) and (29) we come to the diffusion pole of a *weighted* form

$$\phi(\omega, \mathbf{q}) = \frac{g_F/A}{-i\omega + Dq^2}. \quad (31)$$

This expression substantially differs from the relaxation function (14) where the *weight of the diffusion pole* A^{-1} was fixed to unity in order to precisely correspond to the classical diffusion equation $(\partial/\partial t - D\Delta)n(t, \mathbf{r}) = 0$. We see that the diffusion equation is not completely compatible with the developed quantum treatment of the disordered-electron problem, since we have found that the disorder renormalizes not only the diffusion constant D , but also, and more importantly, the diffusion pole itself via its weight $A^{-1} \leq 1$ (the equality applies only in the limit of a clean system).

6. Mean-field theory of the Landau type

In this paragraph we turn to a model evaluation of the diffusion pole weight A^{-1} . But first we investigate low dimensions, $d \leq 2$, where some important conclusions can be made immediately. We have seen that for the relaxation function ϕ to display the diffusion

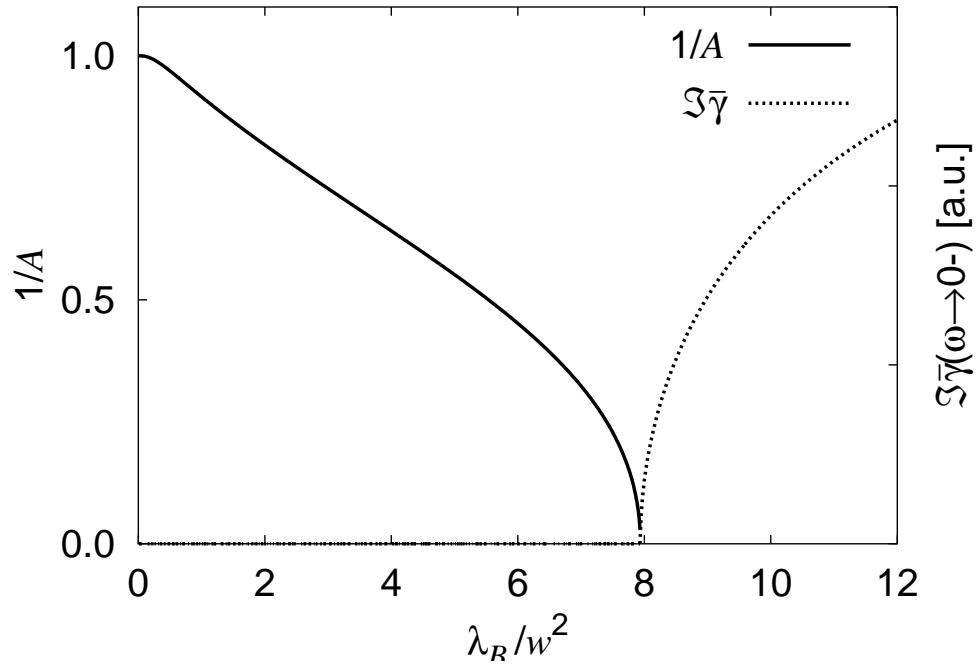


Figure 3: Weight of the diffusion pole A^{-1} and the order parameter in the localized phase $\Im\bar{\gamma}(E_F + i0, E_F - i0)$ calculated from equation (33). We used a semi-elliptic density of states with the bandwidth $2w$, the self-consistent Born approximation for the local vertices, $\lambda, \gamma \rightarrow \lambda_B, \gamma_B$, and set $C_d = 0.1$. Fermi energy E_F lies in the center of the energy band.

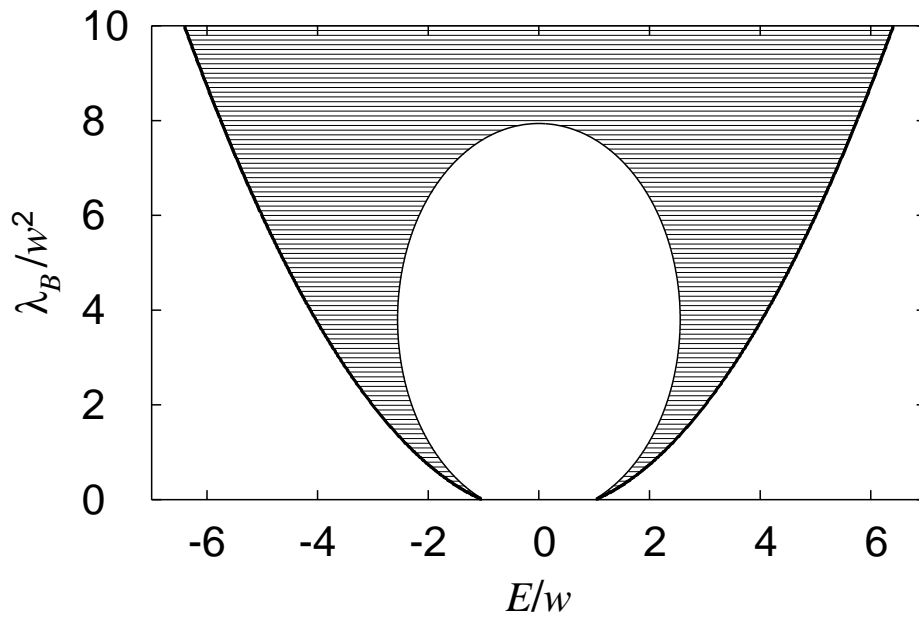


Figure 4: Phase diagram for the same setting as in Figure 3. Thick line is the band edge, hatched area denotes localized states, $\Im\bar{\gamma}(E_F + i0, E_F - i0) \neq 0$.

pole, the same pole has to be present in the ee -irreducible vertex $\bar{\Lambda}^{ee}$. The expression responsible for this non-analytic behavior reads

$$\frac{1}{1 - \bar{\gamma} \bar{\chi}(\mathbf{q})} \sim \frac{1}{-i\omega + Dq^2}. \quad (32)$$

In equation (30), determining the quantity $\bar{\gamma}$, the diffusion pole (32) is integrated over momentum \mathbf{q} . This step represents no difficulty in dimensions $d \geq 3$. On the contrary, in the case of $d \leq 2$ the above pole is not integrable. There can be no $\bar{\gamma}$ fulfilling equation (30) in dimensions $d \leq 2$ if the vertex $\bar{\Lambda}^{ee}$ possesses the diffusion pole. Consequently, our mean-field approximation for two-particle vertices predicts that the diffusive transport cannot take place in low dimensions, $d \leq 2$. This result is in agreement with other treatments [4, 5], which we referred to already in Paragraph 1.

In dimensions $d \geq 3$ the diffusive relaxation is generally possible. Since the diffusion pole in equation (30) is not in higher dimensions as crucial as it is in $d \leq 2$, we can carry out an additional simplification and completely suppress this singularity. Out of the whole geometric series we retain only its first term,

$$\bar{\gamma} = \gamma + \bar{\gamma} \frac{1}{N} \sum_{\mathbf{q}} \frac{\bar{\gamma}^2 \bar{\chi}^2(\mathbf{q})}{1 - \bar{\gamma} \bar{\chi}(\mathbf{q})} \quad \longrightarrow \quad \bar{\gamma} = \gamma + \frac{W^2}{8d} \bar{\gamma}^3 = \gamma + C_d W^2 \bar{\gamma}^3. \quad (33)$$

It is clear that such a reduction is the more acceptable the higher is the spatial dimensionality d . In the model calculations we performed, Figures 3 – 5, the d -dependent constant C_d introduced in equation (33) does not represent its correct high-dimensional value $(8d)^{-1}$. It serves as a free parameter of our approximation instead. It is quite reasonable to set C_d slightly larger than $(8d)^{-1}$, since the simplification performed in formula (33) surely underestimates the right-hand side of the original equation (30).

The cubic equation (33) resembles the Landau mean-field theory of (classical) phase transitions. It has generally three solutions for $\bar{\gamma}(E_F + i0, E_F - i0)$. For sufficiently small disorder strengths, $\gamma < \gamma_c$, all three solutions are real. A perturbative solution is of order γ , while two non-perturbative solutions are of order $\pm W C_d^{1/2}$. The perturbative solution increases and the module of the non-perturbative ones decreases with increasing disorder strength. At a critical randomness $\gamma_c = 2(27C_d W^2)^{-1/2}$ the two positive solutions merge and move into the complex plane for $\gamma > \gamma_c$. Disappearance of real positive solutions for $\bar{\gamma}(E_F + i0, E_F - i0)$ leads to suppression of the diffusion pole and simultaneously to vanishing of the diffusion constant. Quantity $\Im \bar{\gamma}(E_F + i0, E_F - i0)$, emerging beyond the critical point in the localized phase ($\gamma > \gamma_c$), plays the role of an order parameter for the Anderson metal-insulator transition, see Figure 3.

Typical phase diagrams for localized-extended states calculated from formula (33) are plotted in Figures 4 and 5. These figures demonstrate that the localization tendencies are most pronounced close to the band edges and in the impurity band. Results of our mean-field theory are therefore in a nice agreement with the phenomenological picture outlined in Paragraph 1.

7. Weighted diffusion pole vs. conservation laws

It was demonstrated that our construction provides very reasonable results that match phenomenological expectations of how the disordered electrons behave. Before we come to

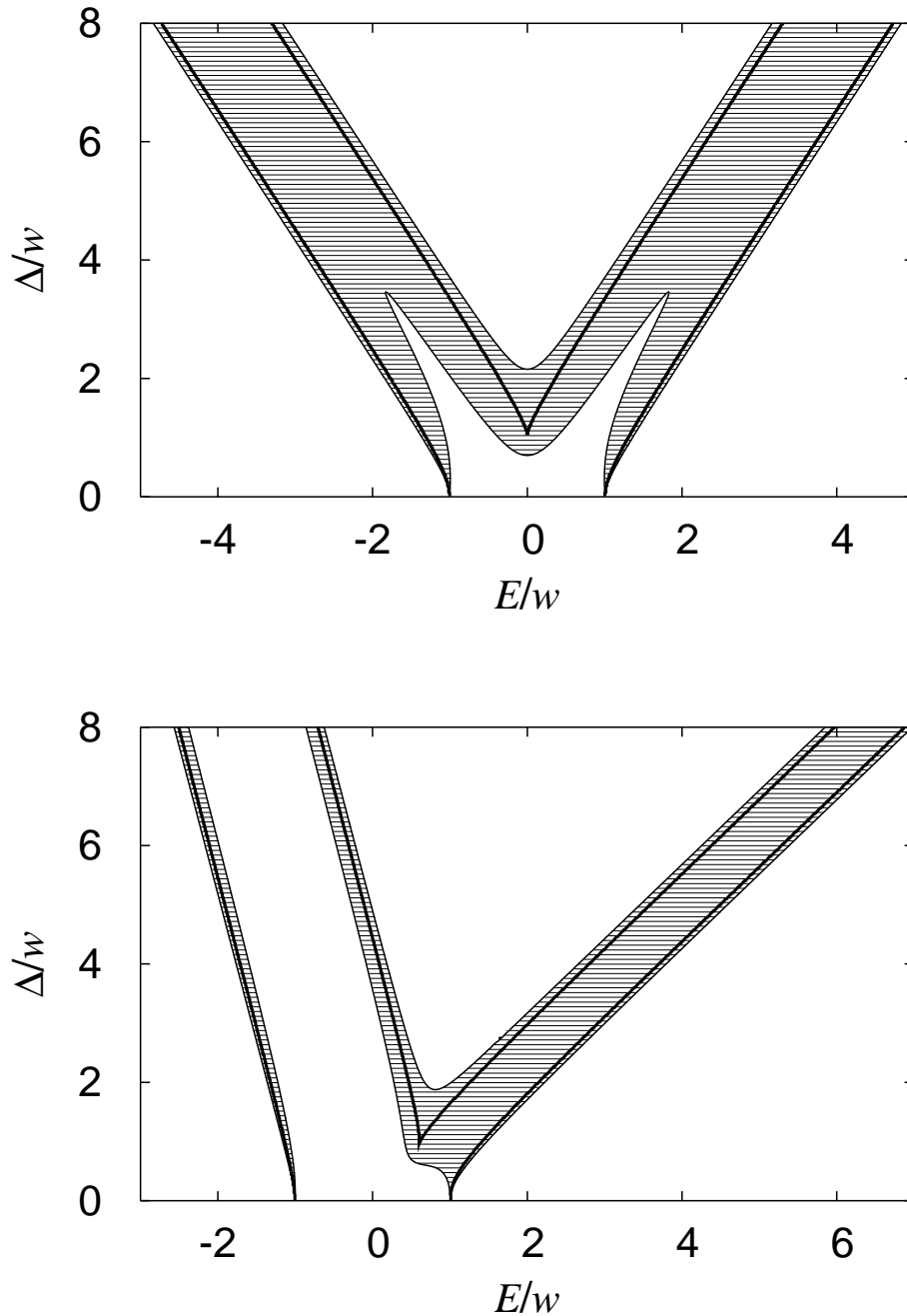
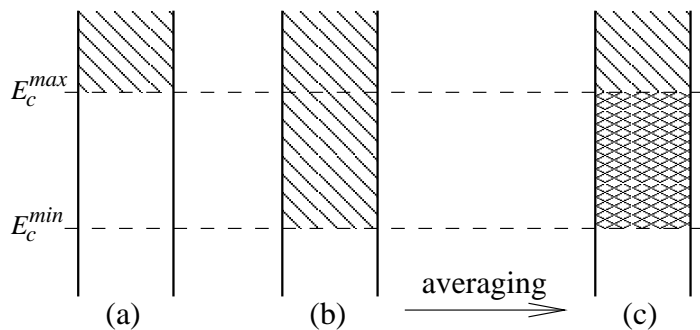


Figure 5: Band and mobility edges in energy-disorder plane for a binary alloy. Thick line is the band edge, region of localized states is hatched. Potential difference between distinct atoms is Δ . The upper pane shows the symmetric case with concentration of both alloy components $c = 0.5$. The lower pane corresponds to an asymmetric alloy with concentration of the minor component $c = 0.2$. It is clear that the tendencies towards localization are enhanced in the impurity band. To calculate these figures we used a semi-elliptic band with the bandwidth $2w$. The parameter C_d was set to $C_d = 1.8$. The extension of the area where $\Im\bar{\gamma}(E_F + i0, E_F - i0) \neq 0$ outside the band is due to incomplete consistency between one- and two-particle functions.

Figure 6: Configurational averaging causes mixing of extended and localized states if the mobility edge E_c is configurationally dependent. Subpictures (a) and (b) represent particular configurations of scattering centers, part (c) depicts configurational average. Hatched regions correspond to localized states. In the doubly hatched energy interval eigenstates of both types are present.



the final conclusions we should comment on one aspect in which our theory substantially differs from other approaches found in the literature. The feature we are about to discuss is the finding that the relevant parameter controlling the transport properties of the system is the weight A^{-1} and not the diffusion constant D . This seems controversial, since the weight A^{-1} should be fixed to unity via the Ward identity [27, 28]

$$\Sigma(z_1, \mathbf{k} + \mathbf{q}) - \Sigma(z_2, \mathbf{k}) = \frac{1}{N} \sum_{\mathbf{k}'} \Lambda_{\mathbf{k}\mathbf{k}'}^{eh}(z_1, z_2; \mathbf{q}) [G(z_1, \mathbf{k}' + \mathbf{q}) - G(z_2, \mathbf{k}')] \quad (34)$$

that expresses the particle number conservation law [29, 19].³ As we have $A^{-1} < 1$ for any non-vanishing disorder, this conservation law is violated in our approximation scheme. Such an inconsistency can be understood in terms of incompleteness of the Hilbert space we work in. The crucial observation is that the localized states cannot be properly described within the formalism based on configurationally averaged (translationally invariant) Green functions. The Hilbert space of a translationally invariant system is spanned over the Bloch-wave basis. In the same time, the localized (spatially confined) electron eigenstates are in the thermodynamic limit orthogonal to the Bloch waves. The weight of the diffusion pole A^{-1} being less than one then means that at a given (Fermi) energy the extended states co-exist with the localized ones that are “invisible” in our treatment due to the above mentioned orthogonality. The mechanism of emergence of the mixed energy intervals is visualized in Figure 6. Analysis of the expression for the relaxation function ϕ , equation (31), shows that there are g_F/A extended (diffusive) states and $g_F(1 - 1/A)$ localized states at the Fermi level E_F .

Because the above explanation of the particle number non-conservation is only verbal, it might be considered insufficient. However, we can offer a formal proof that the Ward identity (34) cannot be fulfilled in principle. From the asymptotic solution for two-particle vertices, formula (29), it follows that the electron-hole irreducible vertex Λ^{eh} displays the so-called *Cooper pole* as it is singular in a point $\mathbf{k}' = -\mathbf{k}$, $\mathbf{q} = \mathbf{0}$ and $\omega = 0$. It can be shown that this singular form is not limited to $d \rightarrow \infty$ but holds in any finite dimensions as well. The Cooper pole in the vertex Λ^{eh} is an image of the diffusion pole in the relaxation function ϕ . Because the vertex Λ^{eh} is non-analytic, the right-hand side of the Ward identity and the selfenergy Σ are also non-analytic. The leading singular

³Quantity Σ standing in equation (34) is the selfenergy, i. e. the one-particle irreducible vertex. Due to length restrictions, the one-particle sector of our approximation is not covered in this abstract. The reader is referred to the full text of the thesis for details on this subject.

behavior of the selfenergy is easily evaluated and reads

$$-\frac{1}{N} \sum_{\mathbf{k}} \frac{\partial \Sigma^R(E, \mathbf{k})}{\partial E} \sim \lim_{\omega \rightarrow 0} K_d \left(\frac{Dk_F^2}{\omega} \right)^2 \left(\frac{|\omega|}{Dk_F^2} \right)^{d/2} \times \begin{cases} 1 & \text{for } d \neq 4l, \\ \ln \frac{Dk_F^2}{|\omega|} & \text{for } d = 4l \end{cases} \quad (35)$$

where k_F is the Fermi momentum and K_d stands for a dimensionless d -dependent constant. This expressions says that in three dimensions the derivative of the selfenergy with respect to its energy argument diverges *everywhere* inside the band. In dimensions $d = 1$ and $d = 2$ the selfenergy itself cannot even be defined. Such a result is clearly unphysical and we are led to a conclusion that we have to give up either the diffusion pole in the relaxation function ϕ or the Ward identity (34). Since without the diffusion pole we lose the physics completely, the only option is to break the Ward identity.

8. Conclusions

A controllable mean-field approximation for two-particle Green functions was derived within the Anderson model of non-interacting electrons moving on an impure lattice. This approximation was motivated and justified by the asymptotic limit to high spatial dimensions. The determination of the approximate two-particle Green functions amounts to solving just a single algebraic equation for a momentum independent quantity $\bar{\gamma}(E_F + i0, E_F - i0)$. For a weak disorder this quantity is real and positive, and the motion of electrons has the diffusive character. When a certain critical disorder strength is exceeded, a nonzero imaginary part $\Im \bar{\gamma}(E_F + i0, E_F - i0)$ emerges. In such a case the electron diffusion is no longer possible. The function $\Im \bar{\gamma}(E_F + i0, E_F - i0)$ plays the role of an order parameter in the transition from diffusive to non-diffusive phase. Achieved results are in agreement with the scenario that is expected to be followed in three and more spatial dimensions — for a weak disorder the electron eigenstates are extended throughout the whole sample, whereas for a strong enough disorder all eigenstates become localized in some finite subvolume.

In the course of development of our theory we discovered a rather surprising fact that we are not able to fully comply with conservation laws represented by Ward identities. A further analysis showed that such an inconsistency is not an artifact of our approximations but is of a considerably deeper origin. In Paragraph 7 we argued that the utilized formalism of configurationally averaged Green functions, which seems to be the only practicable way to tackle the disordered-electron problem by analytical means, is inherently incomplete. The averaging over disorder configurations produces an artificial translationally invariant electronic system, the Hilbert space of which is the one spanned over the Bloch-wave basis. The problems with conservation laws arise from the fact that such a Hilbert space cannot comprehend all the physical phenomena concerning electrons on disordered lattices, since the localized states are orthogonal to this Bloch-wave space in the thermodynamic limit.

References

- [1] N. W. Ashcroft and N. D. Mermin, *Solid state physics* (Holt, Rinehart and Winston, 1976).
- [2] P. W. Anderson, Phys. Rev. **109**, 1492 (1958).
- [3] P. Erdős and R. C. Herndon, Adv. in Phys. **31**, 65 (1982).
- [4] E. Abrahams, P. W. Anderson, D. C. Licciardello, and T. V. Ramakrishnan, Phys. Rev. Lett. **42**, 673 (1979).
- [5] D. Vollhardt and P. Wölfle, in *Electronic Phase Transitions*, edited by W. Hanke and Y. V. Kopayev (Elsevier Science Publishers B.V., Amsterdam, 1992).
- [6] S. V. Kravchenko *et al.*, Phys. Rev. B **50**, 8039 (1994).
- [7] A. Prinz, V. M. Pudalov, G. Brunthaler, and G. Bauer, Superlattices and Microstructures **27**, 301 (2000).
- [8] J. Fröhlich and T. Spencer, Commun. Math. Phys. **88**, 151 (1983).
- [9] И. М. Лифшиц, С. А. Гредескул, Л. А. Пастур, *Введение в теорию неупорядоченных систем* (Наука, Москва, 1982).
- [10] R. J. Elliott, J. A. Krumhansl, and P. L. Leath, Rev. Mod. Phys. **46**, 465 (1974).
- [11] P. Dean, Rev. Mod. Phys. **44**, 127 (1972).
- [12] R. J. Bell, Rep. Prog. Phys. **35**, 1315 (1972).
- [13] P. Soven, Phys. Rev. **156**, 809 (1967).
- [14] B. Velický, Phys. Rev. **184**, 614 (1969).
- [15] P. W. Anderson, E. Abrahams, and T. V. Ramakrishnan, Phys. Rev. Lett. **43**, 718 (1979).
- [16] B. L. Altshuler, D. Khmel'nitzkii, A. I. Larkin, and P. L. Lee, Phys. Rev. B **22**, 5142 (1980).
- [17] R. Kubo, J. Phys. Soc. Japan **12**, 570 (1957).
- [18] R. Kubo, M. Toda, and N. Hashitsume, *Statistical Physics II — Nonequilibrium Statistical Mechanics* (Springer-Verlag, Berlin, 1995).
- [19] V. Janiš, Phys. Rev. B **64**, 115115 (2001).
- [20] K. Ter-Martirosyan, Phys. Rev. **111**, 948 (1958).
- [21] A. D. Jackson, A. Lande, and R. A. Smith, Phys. Rep. **86**, 55 (1982).
- [22] W. Metzner and D. Vollhardt, Phys. Rev. Lett. **62**, 324 (1989).
- [23] A. Georges, G. Kotliar, W. Krauth, and M. J. Rozenberg, Rev. Mod. Phys. **68**, 13 (1996).
- [24] G. Kotliar and D. Vollhardt, Physics Today **57**, 53 (2004).
- [25] V. Janiš and D. Vollhardt, Phys. Rev. B **46**, 15712 (1992).
- [26] V. Janiš, Phys. Rev. Lett. **83**, 2781 (1999).
- [27] D. Vollhardt and P. Wölfle, Phys. Rev. B **22**, 4666 (1980).
- [28] С. В. Малеев, Б. П. Топерверг, ЖЭТФ **69**, 1440 (1975), [S. V. Maleev and B. P. Toperverg, Sov. Phys. JETP **42**, 734 (1975)].
- [29] V. Janiš, J. Kolorenč, and V. Špička, Eur. Phys. J. B **35**, 77 (2003).